Journal of the Physical Society of Japan
Vol. 70, No. 1, January, 2001, pp. 259-266

Mixing-Typed Antiferroquadrupolar Ordering in YbSb

Kenjiro HASHI, Hideaki KITAZAWA[1], Akira OYAMADA[2] and Hiroko ARUGA KATORI

RIKEN (The Institute of Physical and Chemical Research), Wako, Saitama 351-0198
[1]*National Research Institute for Metals (NRIM), Tsukuba, Ibaraki 305-0047*
[2]*Graduate School of Human and Environmental Studies, Kyoto University, Kyoto 606-8501*

(Received June 27, 2000)

Specific heat and magnetization measurements have been performed with a low carrier heavy fermion compound YbSb. Successive phase transitions at 0.5 K and 5 K were observed by specific heat measurements under external magnetic fields up to 12 T. The transition temperature at 5 K increases with increasing external magnetic field. The magnetization measurements indicate the existence of field induced magnetic ordered moments at 5 K. These magnetic properties of the phase transition at 5 K are discussed in terms of a mixing-typed antiferroquadrupolar ordering model with a Γ_6 Kramers doublet as the crystalline electric field ground state.

KEYWORDS: Specific heat, Magnetization, Heavy fermion, quadrupolar ordering, YbSb

§1. Introduction

Yb-monopnictides (YbX: X=N, P, As, Sb) with the NaCl-type crystal structure attract much attention because of their unusual properties which come from the strong competition between the Kondo hybridization and the RKKY interactions.[1)] These compounds are classified to be semimetal and low carrier heavy fermion compounds.[2)] The $(4f)^{13}$ electric configuration ($J = 7/2$) is split by a crystalline electric field (CEF) into a Γ_6 Kramers doublet as the ground state, and a Γ_8 quartet and a Γ_7 doublet as the first and the second exited states, respectively, whose energies correspond to temperatures larger than about 200 K.[3, 4)] In these compounds, neutron diffraction and Mössbauer measurements show that YbN, YbP and YbAs have similar magnetic properties: (1) almost the same antiferromagnetic transition temperatures of about 0.5 K, which is much lower than the Weiss temperature of about −30 K; and (2) the ordered magnetic moment shrink about half from the expected value of 1.33 μ_B for the CEF ground state Γ_6.[5, 6)] On the other hand, in YbSb, these two measurements demonstrated different magnetic properties. Mössbauer spectroscopy reported the presence of two phase transitions of antiferromagnetic and possible antiferroquadrupolar ordering at 0.32 K and 5 K, respectively.[7)] However, neutron diffraction measurements under zero external magnetic field on the same sample did not detect any long range magnetic ordering with magnetic moment larger than 0.1 μ_B down to 7 mK.[5)] As it is proposed by the Mössbauer spectroscopy study, if the phase transition at 5 K is attributed to an antiferroquadrupolar ordering, the different results of Mössbauer spectroscopy and neutron diffraction at 5 K are consistent; because neutron diffraction measurements can never detect quadrupolar ordering without external magnetic field. However, the CEF ground state Γ_6 doublet has no quadrupole moment. Thus, the origin of the phase transitions at 0.32 K and 5 K is controversial. There are relatively fewer studies on YbSb than those on other Yb-monopnictides because of the difficulties in single crystal growth. Some experiments supported the existence of an anomaly at 5 K. It was reported that the specific heat of YbSb shows a small bend at 5 K, which is hardly affected by any external magnetic field up to 10 T.[8)] From NMR measurements, it was proposed that the transition at 5 K is an antiferromagnetic ordering of small moments of about 0.05 μ_B.[9)] From these studies it is clear that YbSb has a phase transition at 5 K, though its nature is not yet determined. On the other hand, there is no other experimental results which confirm the presence of the transition at 0.32 K reported by Mössbauer spectroscopy, so its existence has not been established yet. In this study we have prepared a powder sample of YbSb and performed specific heat and magnetization measurements in order to clarify the presence of the phase transition at 0.32 K and get more information about the phase transition at 5 K. The magnetic properties of the phase transition at 5 K are qualitatively explained by means of a mixing type antiferroquadrupolar ordering model.

§2. Experimental Procedures

A stoichiometric powder sample of YbSb was prepared by a prereaction of the constituent elements in an evacuated and sealed quartz tube at a temperature of up to 700°C. X-ray powder diffraction measurements showed that the crystal structure is of NaCl type with a lattice constant of 6.08 Å, which is consistent with those of the samples used in neutron, Mössbauer spectroscopy and NMR studies. From now on, we refer to the samples prepared by the ETH group, used in NMR measurements and in this study as #1, #2 and #3, respectively.[8, 9)] The full-width at half-maximum (FWHM) of the diffraction line for the {220} plane of #3 is as narrow as that of #2. This means that the homogeneity of sample in #3 is as good as that in #2. A small impurity peak was observed in #3. Judging from the position of the impurity peak, it may come from $YbSb_2$ which is nonmagnetic and shows a

superconductivity below 1.25 K.[10] No anomaly was observed around 1 K in this study as shown below. There were some impurity peaks in #1 and #2. The relative intensity of the impurity peak to the {200} plane for #3 was about 1/100 which is a tenth of those for #1 and #2. This indicates that the purity of #3 is the highest among these samples.

Specific heat measurements were performed down to 0.4 K under external magnetic fields of 0, 6 and 12 T, respectively, by using a commercial microcalorimeter. The temperature dependence of the magnetization was measured in the temperature range between 2 K and 10 K under magnetic fields up to 5 T by a commercial SQUID magnetometer.

§3. Experimental Results

Figure 1 shows the temperature dependence of the specific heat for YbSb #3 under external magnetic fields of 0, 6 and 12 T, respectively. The result of a previous study by Li *et al.* on YbSb #1 was also plotted for comparison.[8] There are two phase transitions at 0.5 K and 5 K. The anomaly at 0.5 K is broad under zero magnetic field, and becomes sharp with increasing magnetic field. It seems that this phase transition at 0.5 K corresponds to the phase transition at 0.32 K reported by the Mössbauer spectroscopy study. The difference in transition temperatures may be due to sample dependence and/or a different way to estimate the transition temperature. In this specific heat measurement the transition temperature of 0.5 K is more reliably obtained as the temperature at the top of the peak, while in the Mössbauer spectroscopy study the transition temperature of 0.32 K was estimated by extrapolating the temperature dependence of the hyperfine field. Thus the existence of a phase transition at 0.5 K is confirmed. However, the behavior of the peak which becomes sharp with increasing magnetic field cannot be explained by a simple antiferromagnetic ordering as proposed by the Mössbauer spectroscopy study.

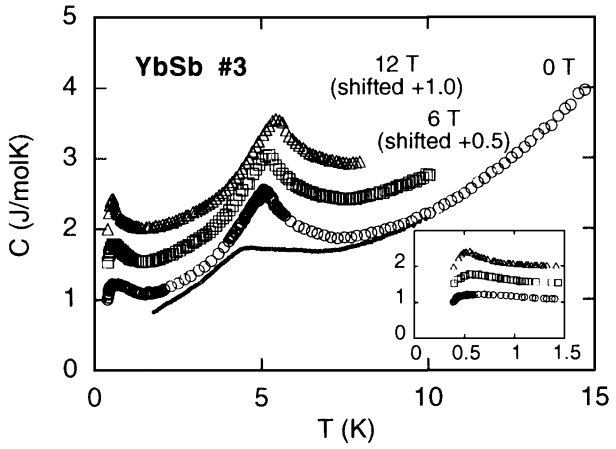

Fig. 1. Temperature dependence of the specific heat for YbSb #3 under external magnetic fields of 0, 6 and 12 T, respectively. Inset shows the lower temperature region. It should be noted that the values of the specific heat for 6 T and 12 T are shifted by +0.5 and +1.0, respectively. The solid line shows the result of a previous study on YbSb #1 under zero magnetic field.[8]

There is a distinct peak at 5 K in the temperature dependence of the specific heat. The second-order like behavior of this peak is observed much more clearly than with YbSb #1. This indicates that the purity of the sample YbSb #3 is better than that of YbSb #1. It seems that the difference of the transition temperatures between YbSb #1 and YbSb #3 is due to sample dependence. The intensity of the peak remains unchanged with magnetic field. Thus, the magnetic entropy is not affected by a magnetic field. Figure 2 shows the magnetic entropy estimated by subtracting the specific heat of LuSb as a nonmagnetic contribution from the observed data of YbSb.[11] The value of the entropy reaches $R\ln 2$ at 10 K which is 20 times higher than the transition temperature of 0.5 K. This behavior is almost the same with those in the other Yb-monopnictides: the entropy of $R\ln 2$ is released at the temperature up to about 20 K which is much higher than the magnetic transition temperature of about 0.5 K.[1] The development of the magnetic short range correlation was observed from 20 K by the inelastic neutron scattering measurement.[12] It seems that these behavior come from the competition between the Kondo hybridization and the RKKY interaction. The value of $R\ln 2$ at 10 K is consistent with the fact that the CEF ground state is a doublet and that excited states exist at energetically much higher levels. In order to get more information about the phase transition at 5 K, we have measured the temperature dependence of the magnetization under various magnetic fields as shown in Fig. 3(a). There is a small bend around 5 K. Below 5 K, M/H measured under a magnetic field of 1 T continue to increase with decreasing temperature, while that measured under 5 T begins to saturate. Figure 3(b) shows the temperature dependence of $\mathrm{d}M/\mathrm{d}T$ under various magnetic fields. The bend around 5 K can be seen more clearly with increasing magnetic field from 1 T to 5 T. Inset of Fig. 3(b) shows the change of the magnetization ΔM at the transition point estimated by extrapolation. Clearly, the magnetization is enhanced below the ordering temperature. This behavior is in accord with the increase of the transition temperature with magnetic field as can be seen from Fig. 1. Figure 4 shows the external magnetic field dependence of the transition temperature in YbSb #3 obtained from the specific heat and

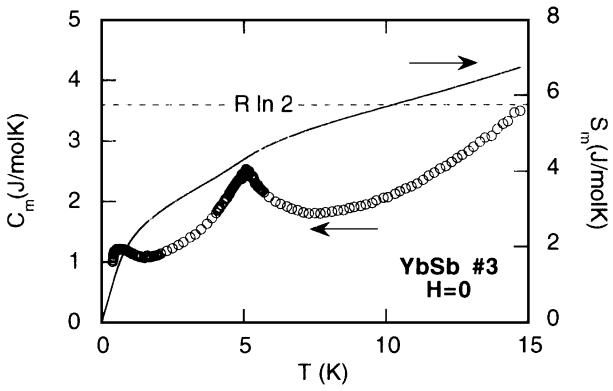

Fig. 2. Temperature dependence of the magnetic specific heat and magnetic entropy for YbSb under zero magnetic field.

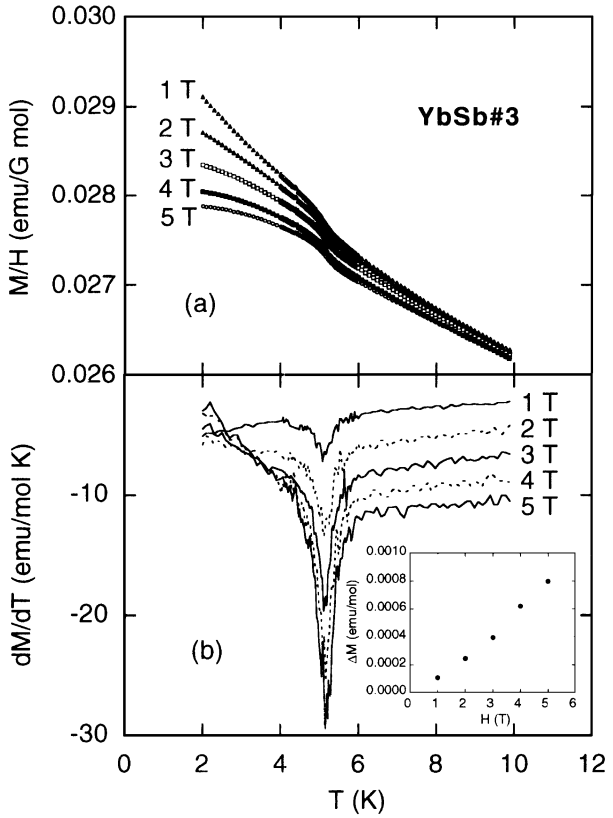

Fig. 3. Temperature dependence of (a) the magnetization M and (b) the $\mathrm{d}M/\mathrm{d}T$ under magnetic fields of 1, 2, 3, 4 and 5 T, respectively. Inset shows the change of the magnetization ΔM at the transition point estimated by extrapolation.

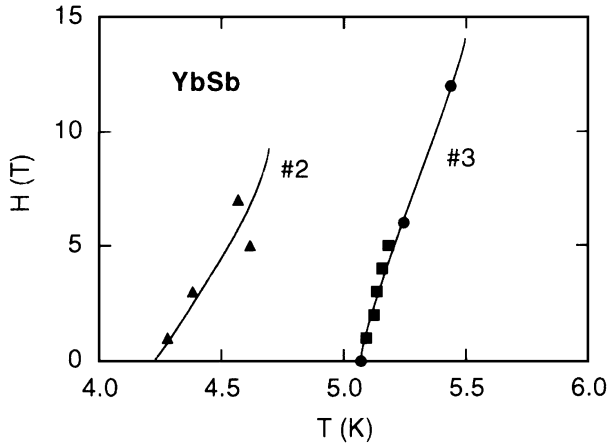

Fig. 4. External magnetic field dependence of the transition temperature obtained from specific heat (solid circle) and magnetization (solid square) for YbSb #3, and from magnetization (solid triangle) for YbSb #2.[9] Solid lines are guides for the eyes.

the magnetization measurements, together with the result on YbSb #2.[9] The transition temperatures increase slightly with increasing magnetic field in both samples, though the absolute values of the transition temperature differ from each other.

The transition temperature increasing with increasing magnetic field and the magnetic component induced by the magnetic field at the transition temperature remind us the antiferroquadrupolar ordering which is typically observed in CeB_6.[13] To the best of our knowledge, all the known antiferroquadrupolar ordering occurs in a compound whose CEF ground state has a quadrupole moment, or where a level with a quadrupole moment is energetically very close to the ground state. YbSb does not satisfy these conditions. However, it was theoretically reported that a quadrupolar ordering can occur by means of a mixing typed quadrupolar interaction between a Kramers doublet ground state and an excited state for $J = 5/2$ by Hanzawa and Kasuya (HK).[14] In the following we apply this theory to YbSb ($J = 7/2$) and show the results of a self consistent numerical model calculation.

§4. Model Calculation

4.1 Model Hamiltonian

According to the HK theory, the total Hamiltonian is written as follows,

$$H_T = H_{CEF} + H_Z + H_{QQ}. \tag{4.1}$$

The first term is the CEF Hamiltonian. The CEF Hamiltonian for a cubic crystal structure is given by

$$H_{CEF} = N\{B_4^0(O_4^0 + 5O_4^4) + B_6^0(O_6^0 - 21O_6^4)\}, \tag{4.2}$$

where N is the number of magnetic ions in a unit, B_4^0 and B_6^0 are CEF parameters and O_n^m are the Stevens operators. The CEF parameters are calculated from the experimentally obtained energy difference of 174 K between the ground state Γ_6 and the first excited state Γ_8, and 453 K between the Γ_6 and the second excited state Γ_7, respectively.[4] Here, we define the total energy difference between Γ_6 and Γ_7 as Δ keeping the ratio of the energy difference between Γ_6 and Γ_8 and between Γ_6 and Γ_7. The second term in eq. (4.1) is the Zeeman Hamiltonian, which can be written as

$$H_Z = -\sum_{i=1}^{N} g_J \mu_{\mathrm{B}} H \cdot J_i, \tag{4.3}$$

where $g_J(= 8/7)$ is the Lande's g-factor, μ_{B} is the Bohr magneton, H is the external magnetic field and J_i is the total angular momentum operator of the i-th site. The third term is the quadrupolar interaction Hamiltonian which can be written in the framework of a two sublattice model considering only an inter-sublattice interaction in the molecular field theory as,

$$H_{QQ} = \sum_{i\in A=1}^{\frac{N}{2}} \{K(\langle u\rangle_B u_i + \langle v\rangle_B v_i) + L(\langle \xi\rangle_B \xi_i + \langle \eta\rangle_B \eta_i + \langle \zeta\rangle_B \zeta_i)\}$$
$$+ \sum_{j\in B=\frac{N}{2}+1}^{N} \{K(\langle u\rangle_A u_j + \langle v\rangle_A v_j) + L(\langle \xi\rangle_A \xi_j + \langle \eta\rangle_A \eta_j + \langle \zeta\rangle_A \zeta_j)\}$$

$$-\frac{N}{2}\{K(\langle u\rangle_A\langle u\rangle_B + \langle v\rangle_A\langle v\rangle_B) + L(\langle \xi\rangle_A\langle \xi\rangle_B + \langle \eta\rangle_A\langle \eta\rangle_B + \langle \zeta\rangle_A\langle \zeta\rangle_B)\}, \tag{4.4}$$

where $\langle\ \rangle_A$ and $\langle\ \rangle_B$ show the mean values for the A- and B-sublattice, respectively, K and L are the coupling constants for the quadrupole moments and u, v, ξ, η, ζ are the quadrupolar operators defined as follows,

$$\Gamma_3: \begin{array}{l} u = J_z^2 - \frac{1}{3}J(J+1), \\ v = (J_x^2 - J_y^2)/\sqrt{3}, \end{array} \tag{4.5}$$

$$\Gamma_5: \begin{array}{l} \xi = (J_yJ_z + J_zJ_y)/\sqrt{3}, \\ \eta = (J_zJ_x + J_xJ_z)/\sqrt{3}, \\ \zeta = (J_xJ_y + J_yJ_x)/\sqrt{3}. \end{array} \tag{4.6}$$

The sum $q_{ll'}$ of the squared matrix elements of the quadrupolar operator o between the CEF eigenstates Γ_l and $\Gamma_{l'}$ is expressed as,

$$q_{ll'} = \sum_{\gamma,\gamma_{l'}} |\langle \Gamma_l\gamma|o|\Gamma_{l'}\gamma_{l'}\rangle|^2, \tag{4.7}$$

and is given in Table I. It should be noted that $\gamma = \alpha, \beta$ denotes the components of Γ_6 and Γ_7, while $\gamma = \kappa, \lambda, \mu, \nu$ the components of Γ_8, respectively. There are no matrix elements within the Γ_6 and Γ_7 doublets, because these are Kramers doublets. The largest element for the Γ_3 component is a mixing typed coupling between the Γ_6 and Γ_8 states, while that for the Γ_5 component is also a mixing typed coupling but between the Γ_7 and Γ_8 states. In the following we consider the next two cases (i) $L = 0$ and $K > 0$ for a Γ_3 coupling, (ii) $K = 0$ and $L > 0$ for a Γ_5 coupling.

At first we consider the effect of a Γ_3 coupling assuming $L = 0$ and $K > 0$. The phase diagram at zero magnetic field is given in Fig. 5(a). The whole transition is of second order. In the quadrupole ordered state, we can find two kinds of self consistent states: (1) U state, in which the quadrupolar moment of u aligns ferrimagnetically and the quadrupolar moment of v is zero, i.e., $\langle u\rangle_A \neq \langle u\rangle_B \neq 0$ and $\langle v\rangle_A = \langle v\rangle_B = 0$; (2) V state, in which one component aligns ferromagnetically and the other aligns antiferromagnetically, *e.g.*, $\langle u\rangle_A = \langle u\rangle_B \neq 0$ and $\langle v\rangle_A = -\langle v\rangle_B \neq 0$. The U state is more stable than the V state at zero magnetic field. The difference in the free energy between these states at zero magnetic field is smaller than that between the U state and the para-state except near the transition temperatures. This character makes the V state to be more stable than the U state under magnetic fields as shown later. Figure 5(b) shows the Δ/K dependence of the weights $n6$ and $n8$ at $k_BT/K = 0.0001$ for the CEF eigenstates Γ_6 and Γ_8, respectively. The weight $n7$ for the Γ_7 state is zero in the region of Δ/K in Fig. 5(b). Both weights $n8$ for Γ_8 at A and B sites decrease continuously with increasing Δ/K and reaches zero at $\Delta_c/K = 182.2$. This means that the U state can be stabilized by a hybridization of the Γ_8 state to the Γ_6 state even if the hybridization is small. The entropy $S(T_c)$ of the system at the transition

Table I. The sum $q_{ll'}$ of the squared matrix elements of the quadrupolar moment o between the CEF eigenstates Γ_l and $\Gamma_{l'}$ for $J = 7/2$ in cubic symmetry.

o	u, v (Γ_3)	ξ, η, ζ (Γ_5)
q_{66}	0	0
q_{77}	0	0
q_{88}	16	36
$q_{67} + q_{76}$	0	46.7
$q_{68} + q_{86}$	140	0
$q_{78} + q_{87}$	12	85.3

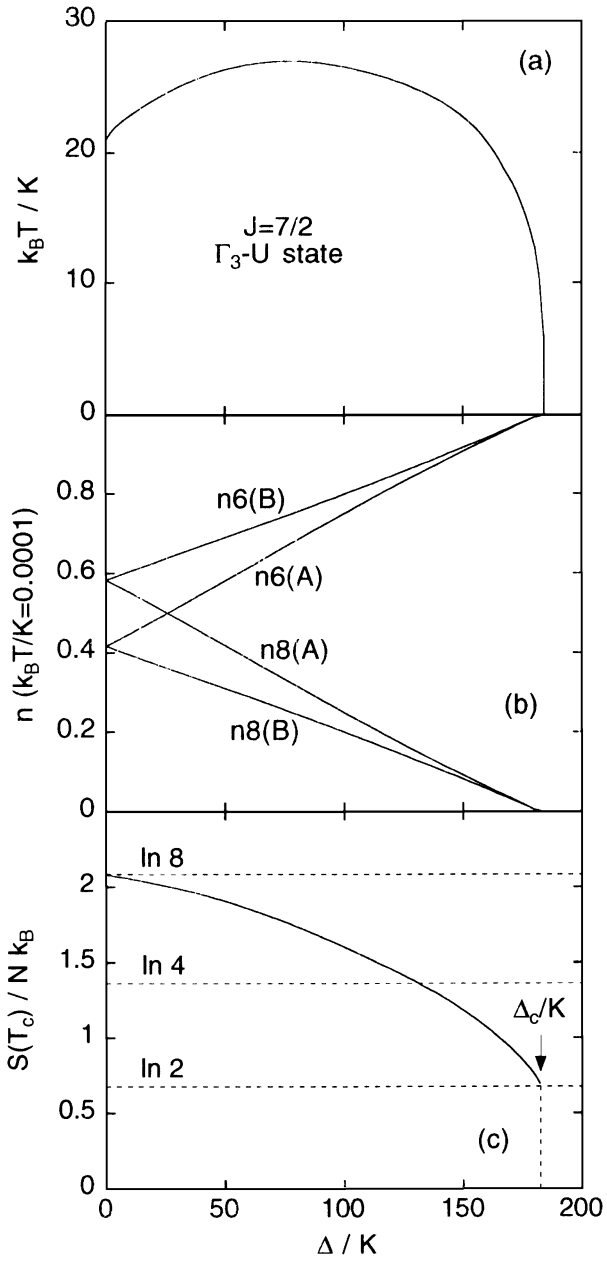

Fig. 5. (a) Phase diagram for a Γ_3 quadrupolar coupling ($K > 0, L = 0$) at zero magnetic field. The whole phase transition is of second order. (b) Δ/K dependence of the weights $n6$ and $n8$ of the Γ_6 and Γ_8 states for the A- and B-sublattice, respectively, at $k_BT/K = 0.0001$. The weight $n7$ of the Γ_7 state is zero in this region of Δ/K. (c) Δ/K dependence of the entropy at the transition temperature T_c.

temperature decreases from $\ln 8$ at $\Delta/K = 0$ to near $\ln 2$ at Δ_c/K continuously as shown in Fig. 5(c). Then, in the Γ_3 coupling case, the second order phase transition of antiferroquadrupolar ordering can occur where the entropy at the transition temperature is near $\ln 2$ for Δ/K near below Δ_c/K. These properties are similar to those for the phase transition around 5 K in YbSb, where the transition is of second order and the entropy including the contribution of a short range ordering is near $\ln 2$.

Next we consider the effect of a Γ_5 coupling assuming $K = 0$ and $L > 0$. We can find three kinds of self consistent quadrupole ordered states: (1) S state, in which one component of the quadrupolar moments of ξ, η, ζ aligns antiferromagnetically and the other components are zero, *e.g.*, $\langle\xi\rangle_A = -\langle\xi\rangle_B \neq 0$ and $\langle\eta\rangle_A = \langle\eta\rangle_B = \langle\zeta\rangle_A = \langle\zeta\rangle_B = 0$; (2) D state, in which two components align antiferromagnetically and the third one aligns ferromagnetically, *e.g.*, $\langle\xi\rangle_A = \langle\eta\rangle_A = -\langle\xi\rangle_B = -\langle\eta\rangle_B \neq 0$ and $\langle\zeta\rangle_A = \langle\zeta\rangle_B \neq 0$; (3) T state, in which three components align ferrimagnetically, $\langle\xi\rangle_A = \langle\eta\rangle_A = \langle\zeta\rangle_A > 0, \langle\xi\rangle_B = \langle\eta\rangle_B = \langle\zeta\rangle_B < 0$. The T state is the most stable among these three states at zero magnetic field. The phase diagram at zero magnetic field is given in Fig. 6(a). The transition for $0 < \Delta/L < 35.9$ is of second order and that for $35.9 < \Delta/L < 38.6$ is of first order. Figure 6(b) shows the Δ/L dependence of the weight $n6$, $n7$ and $n8$ at $k_BT/L = 0.0001$. All the weights $n6$, $n7$ and $n8$ change discontinuously at $\Delta_c/L = 38.6$. The entropy $S(T_c)$ decreases from $\ln 8$ at $\Delta/L = 0$ to near $\ln 2$ at Δ_c/L continuously as shown in Fig. 6(c). Then, in the Γ_5 coupling case, the phase transition is of first order when the entropy at the transition temperature is near $\ln 2$. Thus the properties of the phase transition in YbSb cannot be reproduced by a Γ_5 coupling.

From these considerations a Γ_3 coupling with Δ/K near below Δ_c/K is suitable to reproduce the properties of the phase transition in YbSb. In the following we present the results of a calculation for the Γ_3 coupling with $\Delta/K = 180$ under external magnetic fields and compare with experimental results of YbSb.

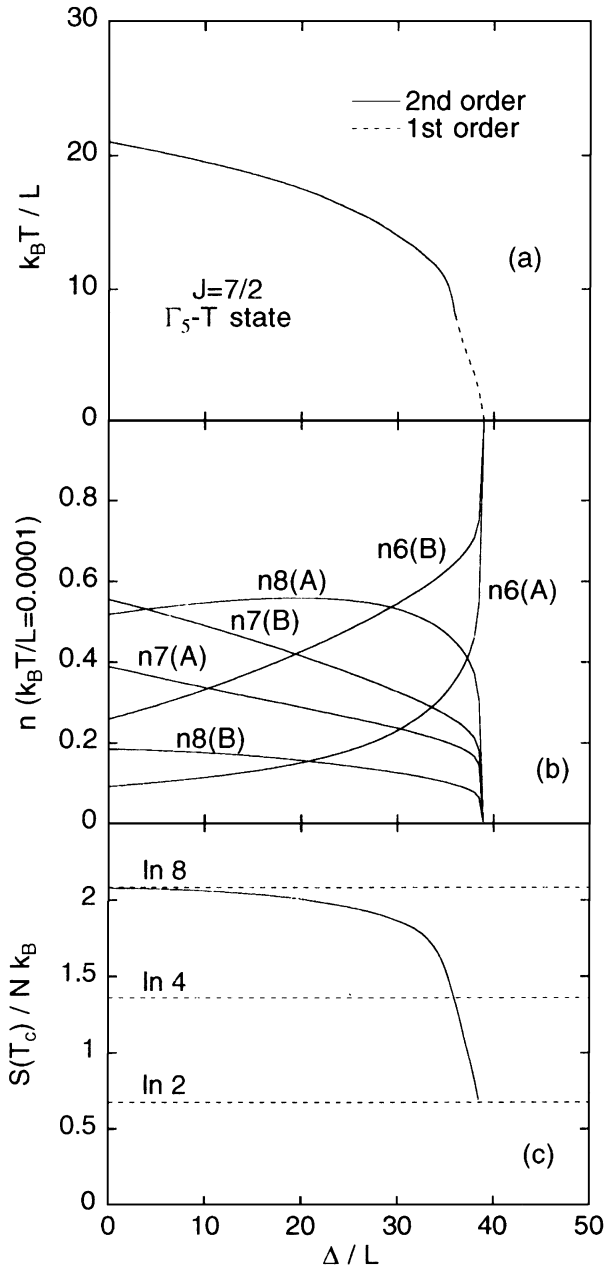

Fig. 6. (a) Phase diagram for the Γ_5 quadrupolar coupling ($K = 0, L > 0$) at zero magnetic field. Solid line shows the second-order phase transition and the broken line the first-order phase transition, respectively. (b) Δ/L dependence of the weights $n6$, $n7$ and $n8$ of the Γ_6, Γ_7 and Γ_8 states for the A- and B-sublattice, respectively, at $k_BT/L = 0.0001$. (c) Δ/L dependence of the entropy at the transition temperature T_c.

4.2 Calculated results under magnetic field and comparison with experimental results

The phase diagram for the Γ_3 coupling with $\Delta/K = 180$ under a magnetic field along the [001] axis is shown in Fig. 7. In the whole ordered state the U state is more stable than the V state. The whole transition is of second order. The transition temperature increases with increasing magnetic field up to about $\mu_BH/K = 10$. Figure 8(a) shows the temperature dependence of the specific heat calculated under magnetic fields of $\mu_BH/K =$ 0, 1, 3 and 5, respectively. The specific heat under zero magnetic field shows a small peak at the transition temperature of 13.2 corresponding to the antiferroquadrupolar ordering. This peak grows with increasing magnetic field. The calculated specific heat under magnetic field shows two additional peaks, one broad and the other sharp, at temperatures lower than the transition temperature. The broad peak shifts to higher temperature with increasing magnetic field. This peak seems to correspond to the Schottky peak due to the Zeeman splitting of the quadrupolar ordered state by the external magnetic field. On the other hand, the sharp peak becomes stronger with increasing the magnetic field. This peak cannot be explained by the Schottky peak. This peak is ascribed to the crossover within the U state from the state which gains the energy mainly by the quadrupole interaction at higher temperatures to the state which gains the more energy by the Zeeman interaction and the CEF energy at lower temperatures. Indeed, the calculated magnetization shows an increase below the temperature which corresponds to this sharp peak as shown later. This peak may be associated with the peak ob-

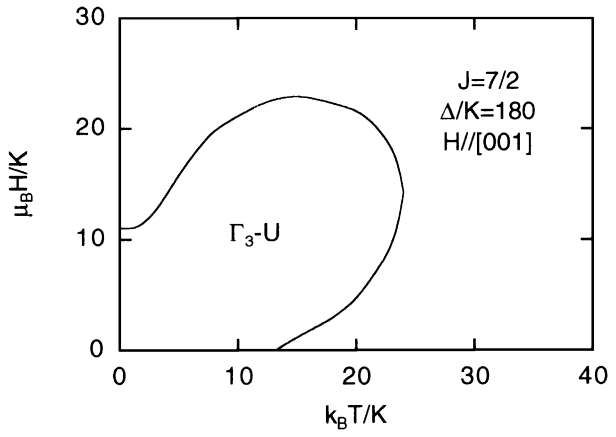

Fig. 7. Phase diagram for the Γ_3 coupling with $\Delta/K = 180$ under a magnetic field along the [001]-axis. All phase transitions are of second order.

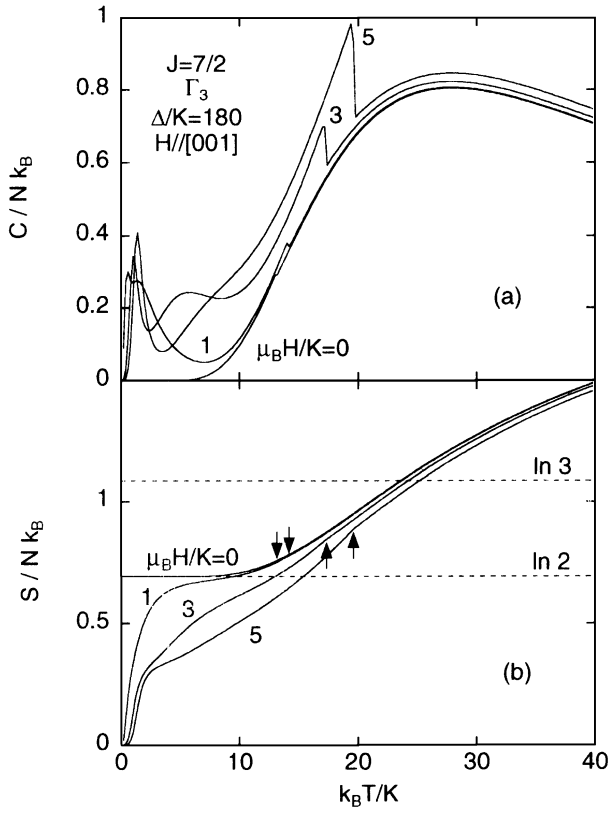

Fig. 8. Temperature dependence of (a) the specific heat and (b) the entropy calculated under magnetic fields of $\mu_B H/K = 0$, 1, 3 and 5, respectively, along the [001]-axis for the Γ_3 coupling with $\Delta/K = 180$. Arrows show the transition points.

served around 0.5 K in YbSb, though it is observed under zero magnetic field in YbSb. This difference at zero magnetic field may originate from the fact that no magnetic interaction is included in the present calculation. Figure 8(b) shows the temperature dependence of the entropy calculated under magnetic fields of $\mu_B H/K = 0$, 1, 3 and 5, respectively. The calculated entropy at the transition temperature is near ln 2 and almost independent of the magnetic field. These properties are consistent with

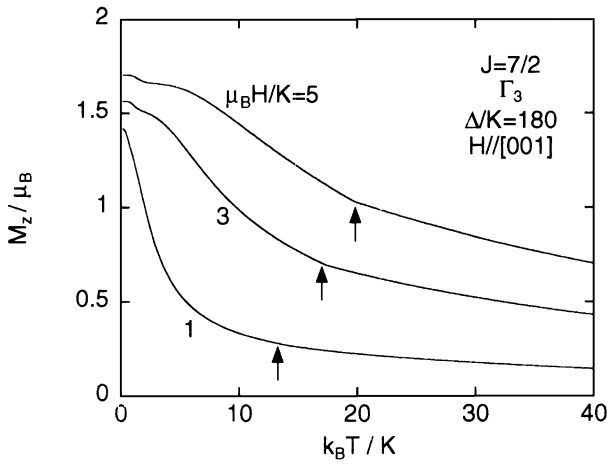

Fig. 9. Temperature dependence of the magnetization $M_z = g_J(\langle J_z\rangle_A + \langle J_z\rangle_B)/2$ calculated under magnetic fields of $\mu_B H/K = 1$, 3 and 5, respectively, along the [001]-axis for the Γ_3 coupling with $\Delta/K = 180$. Arrows show the transition points.

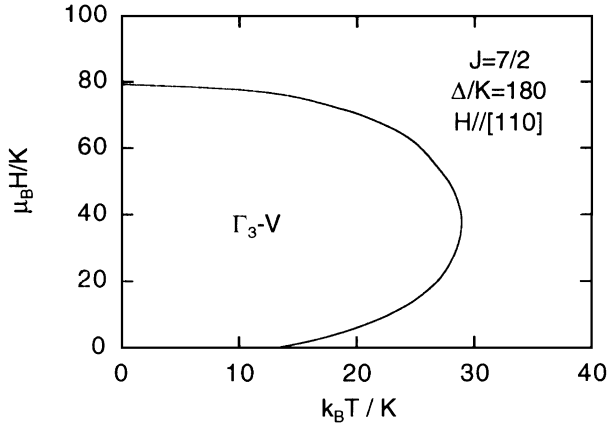

Fig. 10. Phase diagram for the Γ_3 coupling with $\Delta/K = 180$ under a magnetic field along the [110]-axis. All phase transitions are of second order.

experimental results. The temperature dependence of the magnetization $M_z = g_J(\langle J_z\rangle_A + \langle J_z\rangle_B)/2$ calculated under magnetic fields of $\mu_B H/K = 1$, 3 and 5, respectively, are shown in Fig. 9. The magnetization shows a small bend at the transition temperature, which becomes clearer with increasing magnetic field. The magnetization under $\mu_B H/K = 1$ continues to increase down to the lowest temperature, while that under $\mu_B H/K = 5$ begins to saturate below the transition temperature. These behaviors are consistent with experimental results.

The phase diagram for the Γ_3 coupling with $\Delta/K = 180$ under a magnetic field along the [110] axis and the [111]-axis are shown in Fig. 10 and Fig. 11, respectively. For a field along the [110] axis the V state is more stable than the U state in the whole ordered state and the whole transition is of second order. For a field along the [111]-axis the U state is stable under lower field, while the V state become stable under higher field. The whole transition is of second order. The calculated transition temperature increases with increasing magnetic fields both

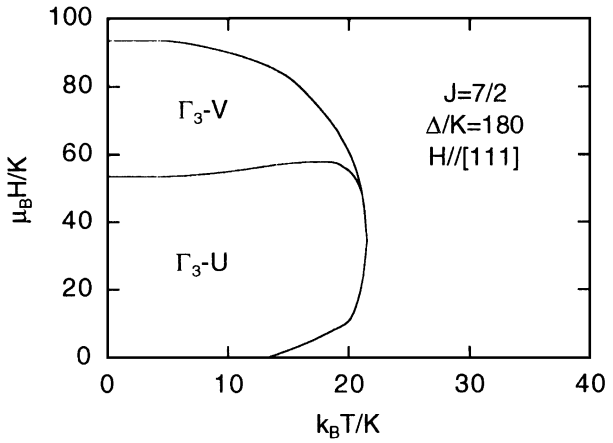

Fig. 11. Phase diagram for the Γ_3 coupling with $\Delta/K = 180$ under a magnetic field along the [111]-axis. All phase transitions are of second order.

along the [110] and the [111] axes as in the case along the [001]-axis mentioned above. The observed transition temperature around 5 K increases with increasing magnetic field in a powder sample. This behavior can be reproduced qualitatively by the present model.

§5. Discussion and Conclusion

As mentioned in §4, the magnetic properties of the phase transition at 5 K in YbSb are qualitatively well reproduced by a model calculation for a mixing typed antiferroquadrupolar ordering. This model suggests that the characteristic parameter Δ/K in YbSb is nearly below Δ_c/K. This can explain the fact that the other Yb-monopnictides show no additional phase transition except for an antiferromagnetic phase transition around 0.5 K, because the magnitude of the CEF splitting Δ for YbSb is the smallest among the Yb-monopnictides. In other words, other Yb-monopnictides have larger Δ/K values than Δ_c/K. However, it seems that the quadrupolar interaction has large influence on the magnetic properties of the Yb-monopnictides. Using eq. (4.7), the sum $q_{ll'}$ of the squared matrix elements of the quadrupolar moment o between the CEF eigenstates for $J = 5/2$ in a cubic symmetry is listed in Table II, which is corresponding to the case for cubic Ce compounds such as CeB_6. In the present model calculation for YbSb, the Γ_3 type quadrupolar interaction plays an important role. The matrix element for this interaction, $q_{68} + q_{86}$ listed in Table I, is about 4 times larger than the largest element for $J = 5/2$, $q_{78} + q_{87}$ for the Γ_5 type interaction listed in Table II. Then, it seems that the quadrupolar interaction has large influence on the magnetic properties in Yb-monopnictides though their CEF ground state is a Kramers doublet. The Yb monopnictides except YbSb have a broad peak in the specific heat around 5 K, whose origin is not clear.[8] This broad peak is hardly affected by any magnetic field up to 10 T. This peak may be associated to the development of a short range correlation of the antiferroquadrupole moments. Indeed, in these compounds the anomalous splitting of the first excited state Γ_8 is observed by the neutron spectroscopy.[15, 16]

Table II. The sum $q_{ll'}$ of the squared matrix elements of the quadrupolar moment o between the CEF eigenstates Γ_l and $\Gamma_{l'}$ for $J = 5/2$ in cubic symmetry.

o	u, v (Γ_3)	ξ, η, ζ (Γ_5)
q_{77}	0	0
q_{88}	28.4	1.78
$q_{78} + q_{87}$	8.89	35.6

Unfortunately, it is hard to perform quantitative comparison of the calculated results with experiments due to the following reason. The value of Δ/K must be nearly below Δ_c/K so that the entropy at the transition temperature is near $\ln 2$. For YbSb the value of Δ is reported to be 453 K, then the value of K is estimated to be about 2.5 K assuming the Δ/K to be 180 ($\Delta_c/K \approx 182.2$). When Δ/K is close to Δ_c/K, the transition temperature strongly depends on Δ/K as shown in Fig. 5(a). For example, $\Delta/K = 182.240$ gives a transition temperature $k_B T/K$ of 5.8, while $\Delta/K = 182.242$ gives no phase transition under zero magnetic field. Then it is hard to choose the value of Δ/K so as to make $k_B T/K = 2$ corresponding to a transition temperature of 5 K for YbSb.

In conclusion, specific heat and magnetization measurements have been performed with a low carrier heavy fermion compound YbSb. The successive phase transitions around 0.5 K and 5 K were observed by specific heat measurements under external magnetic fields up to 12 T. The presence of a phase transition around 0.5 K which is proposed by the Mössbauer spectroscopy study is confirmed. The transition temperature of around 5 K increases with increasing external magnetic field. Magnetization measurements indicate a clear enhancement of the uniform component of magnetic moment below 5 K. These magnetic properties of the phase transition are discussed in terms of a mixing-typed antiferroquadrupolar ordering model with the Γ_6 doublet as the CEF ground state. The magnetic phase diagram and the temperature dependence of the specific heat and the magnetization were obtained by numerical calculations in the framework of a two sublattice model in the mean field theory. The magnetic properties of the phase transition around 5 K in YbSb are qualitatively reproduced by the calculation. It suggests that the phase transition around 5 K in YbSb is an antiferroquadrupolar ordering of mixing type even if the CEF ground state is a doublet and the first excited state Γ_8 is located above 174 K. The discrepancy between the experimental results of the neutron diffraction and the Mössbauer spectroscopy can be solved by introducing the mixing typed antiferroquadrupolar interaction.

Acknowledgements

The authors would like to thank Dr. K. Katsumata of RIKEN for the use of the microcalorimeter. One of the authors (K. H.) would like to thank Dr. T. Mutou of RIKEN for fruitful discussions. One of the authors (K. H.) is supported by the Special Postdoctral Researchers Program of RIKEN.

1) H. R. Ott, H. Rudigier and F. Hulliger: Solid State Commun. **55** (1985) 113.
2) A. Oyamada, C. Ayache, T. Suzuki, J. Rossat-Mignod and T. Kasuya: J. Magn. Magn. Mater. **90&91** (1990) 443.
3) M. Kohgi, K. Ohoyama, A. Oyamada, T. Suzuki and M. Arai: Physica B **163** (1990) 625.
4) A. Dönni, A. Furrer, P. Fischer, F. Hulliger and P. Wachter: Physica B **171** (1991) 353.
5) A. Dönni, A. Furrer, P. Fischer, F. Hulliger, P. Wachter and H. R. Ott: J. Magn. Magn. Mater. **90&91** (1990) 143.
6) P. Bonville, J. A. Hodges, F. Hulliger, P. Imbert, G. Jéhanno, J. B. Marimon da Cunha and H. R. Ott: J. Mag. Mag. Mater. **76&77** (1988) 473.
7) P. Bonville, J. M. Broto, A. Fert, F. Gonzalez-Jimenez, A. Hamzic, F. Hulliger, P. Imbert, G. Jéhanno, J. B. Marimon da Cunha, M. Miljak and H. R. Ott: J. Phys. Collq. **49** (1988) 727.
8) D. X. Li, A. Oyamada, H. Shida, T. Suzuki, T. Kasuya, A. Dönni and F. Hulliger: Physica B **186–188** (1993) 547.
9) K. Hashi, A. Oyamada, S. Maegawa, T. Goto, D. X. Li, T. Suzuki, A. Dönni and F. Hulliger: Physica B **259–261** (1999) 159.
10) Y. Yamaguchi, S. Waki and K. Mitsugi: J. Phys. Soc. Jpn. **56** (1987) 419.
11) R. J. Birgeneau, E. Bucher, J. P. Maita, L. Passell and K. C. Turberfield: Phys. Rev. B **8** (1973) 5345.
12) K. Ohoyama, T. Osakabe, A. Dönni, M. Kohgi, A. Oyamada and T. Suzuki: Physica B **213&214** (1995) 119.
13) J. M. Effantin, J. Rossat-Mignod, P. Burlet, H. Bartholin, S. Kunii, T. Kasuya: J. Magn. Magn. Mater. **47&48** (1985) 145.
14) K. Hanzawa and T. Kasuya: J. Phys. Soc. Jpn. **53** (1984) 1809.
15) K. Ohoyama, M. Kohgi, T. Nakane, M. Arai, A. D. Taylor, A. Oyamada and T. Suzuki: Physica B **180&181** (1992) 250.
16) L. Keller, W. Henggeler and A. Furrer: Europhys. Lett. **26** (1994) 353.